Using comb-like instrumental functions in high-resolution spectroscopy

A S Kaminskii††‡, E L Kosarev§‖ and E V Lavrov†¶

† Institute of Radioengineering and Electronics, Russian Academy of Sciences,
11 Mokhovaya Street, Moscow 103907, Russia
§ P L Kapitza Institute for Physical Problems, Russian Academy of Sciences,
ul.Kosygina, 2, Moscow 117334, Russia

Abstract. A new method is presented for the analysis of spectra from
spectrometers with a complicated instrumental function such as a comb-like one
which may be represented as a sum of several narrow peaks shifted relative to one
another. The method is based on the solution of the convolution integral equation
using the signal restoration procedures employed in the software package
RECOVERY. It is implemented for the case of a spectrometer consisting of a
scanning Fabry–Pérot interferometer and a grating monochromator having equal
rates of scanning. The efficiency of the procedure is demonstrated by applying it to
the photoluminescence (PL) spectra of excitons bound to the isoelectronic
hydrogen-related centres in silicon grown in a hydrogen atmosphere. It is shown
that the spectral density of the analysed radiation is resolved successfully and that
the spectrometer has effectively a greater working range and signal-to-noise ratio
in comparison with the standard Fabry–Pérot interferometer. The procedure can be
used in any kind of high-resolution spectroscopy (optical, x-ray, neutron, etc).

1. Introduction

Any spectral instrument introduces distortions in an analysed spectrum. It is well known (see for example [1–7]) that under the general assumptions defined below the output signal $F(x)$ of any linear spectrometer is the sum of the integral $F_0(x)$, the distortion introduced by the spectrometer, and the noise $N(x)$ which is always present in the output of a real spectrometer

$$F(x) = F_0(x) + N(x) \qquad (1)$$

where

$$\int_a^b K(x, y)G_0(y)\, \mathrm{d}y = F_0(x) \qquad c \leq x \leq d. \qquad (2)$$

In equation (1) we assume that the noise is not correlated in successive measurement points and that it is additive with the signal. If this is not the case (for instance in Poissonian noise), (1) can be considered as a definition of a random function, $N(x)$, which equals in this case the difference between the random output signal and the integral $F_0(x)$. In both cases we also assume that $F(x)$ does not contain systematic errors, i.e. $\overline{N(x)} = 0$.

‡ E-mail address: kam@mail.cplire.ru
‖ E-mail address: kosarev@kapitza.ras.ru
¶ E-mail address: lav@mail.cplire.ru

In equation (2), $F_0(x)$ represents the signal which would be on the output of the spectrometer in the absence of noise, $K(x, y)$ is the instrumental function of the spectrometer and $G_0(y)$ is the spectral density of the analysed radiation which is the subject of the reconstruction procedure. The integration is performed over the interval (a, b) in which $K(x, y)$ is different from zero. The interval (c, d) gives the limits of the wavelength range.

It can be seen from (1) and (2) that if noise is present, $G_0(y)$ cannot be recovered exactly. In this case all that we can hope for is to find a function $G(y)$ which is the optimal or near-optimal estimation of $G_0(y)$ in some statistical sense.

If the noise is absent, reconstruction of the spectral density of the analysed signal is reduced to the solution of the integral equation (2) which, in this case, can be solved exactly.

When the noise is small, and the instrumental function (kernel of equation (2)) is close to the δ-function

$$K(x, y) \approx \delta(x - y)$$

the spectrometer itself solves the problem and the output signal approximately equals the spectral density of the analysed radiation, i.e.

$$F(x) \approx G_0(x).$$

If the instrumental function of the spectrometer is noticeably wider than the features of a spectrum or if it has a complicated form (e.g. several overlapping peaks), the output signal can differ very distinctly from $G_0(x)$ and its reconstruction from the measured function $F(x) \approx F_0(x)$ necessitates the solution of the integral equation (2).

In real situations there is always noise on the output of a spectrometer and the instrumental function differs appreciably from a δ-like function. In this case $F(x)$ is a random function and for reconstruction of the solution $G_0(y)$ from equations (1) and (2) we have to take into account both that the signal is random and that the problem (1), (2) may fall into the set of ill-posed problems [2]. We note that the extent to which the problem is a well- or ill-posed one is determined mainly by the kernel in the integral operator (2). The randomness of the input data introduces further difficulties to the problem of signal reconstruction. The software for signal recovery from noisy data used in this paper is based on the maximum likelihood principle [7] and it takes into account both of these circumstances. A more detailed description of this software is given in section 3 of this paper. We would like to note here that the quality of restoration of $G_0(y)$, i.e. the difference between $G(y)$ and $G_0(y)$, depends on many factors, among which are the profile of the instrumental function, the value of the signal-to-noise ratio and the method of restoration.

As a rule, we use spectrometers with a narrow instrumental function with one brightly expressed peak. In this case the spectrum recorded reflects the main features of the analysed spectrum. Even in this case the use of restoration programs can increase the spectral resolution appreciably and reveal additional structures in a spectrum. If the instrumental function is fairly complicated (e.g. it has a number of well resolved maxima), the measured spectrum $F(x)$ will differ significantly from the analysed spectrum.

In the present paper we show that the solution of the inverse problem for a spectrometer with a complicated instrumental function permits the successful reconstruction of the unknown spectrum and gives an opportunity for substantial enhancement of the performance of standard spectral equipment (for example, use of a Fabry–Pérot interferometer in large spectral intervals without reduction of its resolving power). We stress that such an enhancement of the resolving power of a spectrometer is actually impossible to achieve without the use of computer programs.

2. The spectrometer

The basic ideas outlined in the introduction were realized experimentally in a spectrometer that consists of a scanning Fabry–Pérot interferometer and a scanning grating monochromator. It is shown schematically in figure 1. The detector is a cooled photomultiplier tube (PMT) operating in photon counting mode. The spectrometer is controlled by the unit of control and data acquisition (UCDA) connected to a personal computer (PC).

The analysed radiation passes through the interfero-meter and the grating monochromator and it is then detected by the PMT. Voltage pulses arising on the PMT load are
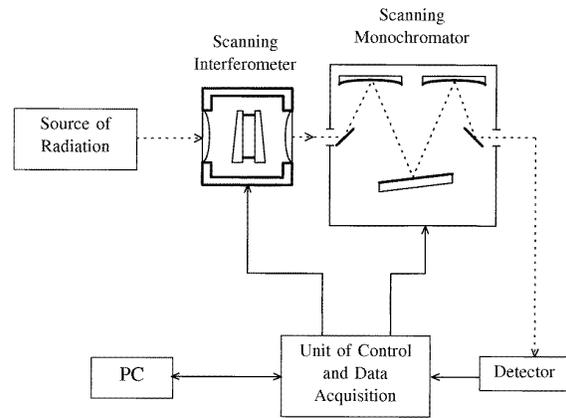
Figure 1. Schematic diagram of the spectrometer. Broken lines show the path of the analysed light. Full lines show communications between different blocks of the spectrometer.

registered by a counter located in the UCDA and recorded into a PC file.

For fine filtering of the radiation we used a scanning Fabry–Pérot interferometer with a fixed distance of 1 mm between mirrors placed in a chamber filled with CO_2 gas. The interferometer mirrors have a multilayer dielectric cover with a reflection coefficient of $\sim$85–90% at $\lambda \sim 1$ μm. The spectral resolution (FWHM) and energy separation between the orders of interference was 30 μeV (0.24 cm^{-1}) and 620 μeV (5 cm^{-1}) respectively. The gas pressure in the interferometer chamber could be changed from 0 to 5 atm. and was controlled by an absolute pressure gauge. The value of the pressure was monitored by the UCDA and recorded into a PC file.

The instrumental function of the interferometer obtained by recording of the very narrow line at $\lambda = 1.15$ μm from a helium–neon laser is shown in figure 2(a). The use of such an interferometer for the spectral analysis allows the scanning of spectra contained in a narrow spectral interval, approximately equal to the distance between the nearest orders of interference.

For coarse filtering of the radiation we use the scanning grating monochromator with a linear dispersion of 4 nm mm^{-1}. Spectral scanning is achieved by rotating the diffraction grating (600 lines per mm) by discrete angle steps $\Delta\Phi$ using a stepping motor with an appropriate speed setting. This permits us to set the scanning rates of both the monochromator and the interferometer to be equal. The instrumental functions of the monochromator obtained by recording the helium–neon laser line at $\lambda = 1.15$ μm for two slit widths (0.12 mm and 0.4 mm) are shown by broken curves in figures 2(b) and (c) respectively.

The scanning of spectra is performed in the following way. First of all the scanning rates of the monochromator and interferometer are set to be equal to each other. In this case we have $K(x, y) = K(x - y)$. The monochromator with a fixed slit width is then tuned at the initial point of the spectral interval to be analysed. We may choose a symmetrical instrumental function of spectrometer (see figures 2(b) and (c)) by changing the initial pressure and
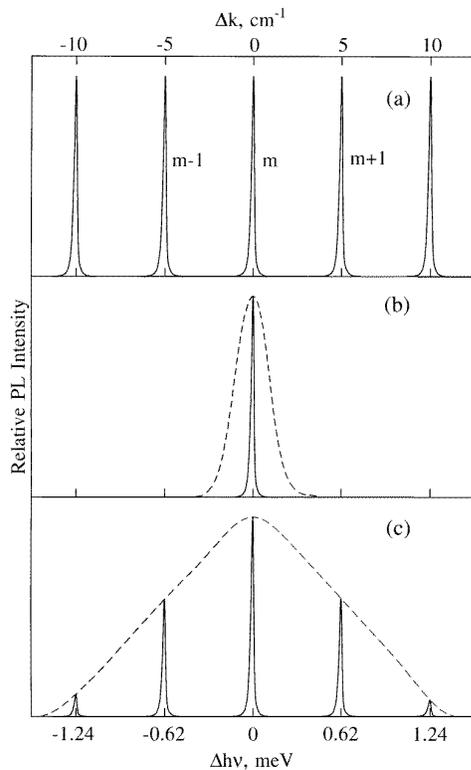
Figure 2. Instrumental functions used for spectral density recovery: (a) is the instrumental function of the Fabry–Pérot interferometer; (b) and (c) are the instrumental functions of the grating monochromator (broken curves) and the instrumental functions of the spectrometer (full curves) for slit-widths equal to 0.12 mm and 0.4 mm respectively. The instrumental functions of the spectrometer were obtained by multiplying appropriate instrumental functions of the monochromator and the interferometer, m is the order of interference. The distance between marks equals the energy distance between the nearest orders of interference (in this case, it is 0.62 meV or 5 cm^{-1}).

by controlling the pressure change ΔP, angle $\Delta \Phi$ and time interval Δt with the UCDA and PC while the counter registers pulses from the PMT. The spectrometer then begins the scanning procedure. When the interferometer and the monochromator have performed one step the UCDA turns on the counter for a time interval Δt. The UCDA initiates a new step until the spectrometer has completed the scan of one order of interference. At this moment the UCDA stops the monochromator and returns the interferometer to the initial state. The cycle is repeated until the spectrometer has covered the whole spectral interval under analysis.

The spectrometer may be used in many modes. We describe here only two of them, i.e. when

$$K(x, y) = K(x - y).$$

In this case equation (2) is a convolution integral.

In the first mode the width of the monochromator slit is narrower than the interval by one order of interference and therefore the spectrometer has the δ-like instrumental function shown in figure 2(b) by the full curve. Typically, the spectrum recorded by the spectrometer in this mode

is close to the analysed spectrum, and its analysis can be carried out in a wide spectral interval. The main drawback of this mode is the need to use a very narrow monochromator slit width. This results in a sharp decrease of the signal-to-noise ratio. For this reason we consider further a more appropriate mode of operation.

In the second mode the monochromator slit width is chosen reasonably large to increase the intensity of detected light and the signal-to-noise ratio. In this case several orders of interference fall into a spectral interval that corresponds to the slit width. The instrumental function then has the comb-like form shown in figure 2(c). This function may be obtained by multiplying the instrumental functions of the interferometer and the monochromator. It should be noted that the maximum number of peaks in the instrumental function (and hence signal-to-noise ratio) is restricted by the accuracy in movement of the diffraction grating and the discrepancy between the instrumental function used for restoration and a real one. In our case it was found that the instrumental function with five peaks is optimal.

It will be shown that the recorded spectrum differs markedly from the analysed spectrum in all spectral intervals because in this mode several spectral intervals are analysed simultaneously. Consequently, the use of computer programs for signal restoration becomes inevitable. As the signal-to-noise ratio in this mode is to be improved, it is reasonable to expect that the restoration procedure will not only restore the analysed spectrum, but will also increase the resolving power of the spectrometer.

3. The procedures for signal recovery

In this section we consider only the main points of the used procedures for signal recovery and we address readers to a more detailed discussion of this subject in [6] and [7]. In order to solve the integral equation (2) with random right-hand side data we use the program DCONV from the program package RECOVERY [7]. All programs from this package are based on the maximum likelihood method (MLM) because this method retains the capability for attaining the superresolution limit.

Let us introduce first some useful definitions concerning the superresolution. The resolution of any linear device with the instrumental function $K(x)$ can be defined as the effective width of this function, i.e.

$$\Delta = \int_{-\infty}^{\infty} K^2(s) \, ds \qquad s = x - y \qquad (3)$$

providing the normalizing condition at the origin $K(0) = 1$.

The resolution of spectral devices can be improved in comparison to Δ using modern techniques for solving integral equations, thus superresolution is achieved. We define the superresolution factor as the ratio of Δ to the separation δ between two narrow lines which can be distinguished after the deconvolution procedure

$$SR = \Delta/\delta. \qquad (4)$$

We note that Rayleigh's definition of resolution yields $\delta = \Delta$, so in this case the superresolution factor is $SR = 1$. When the resolution is improved mathematically, $SR > 1$. The improvement is always limited by noise. At zero noise an exact solution of equation (2) can be found, which corresponds to an infinite superresolution.

The highest possible superresolution factor is closely related to Shannon's theorem about the highest possible transmission rate of information through a noisy channel [6]. When a spectrum is not parametric, i.e. the function we want cannot be described by a simple formula with a few parameters, the limiting superresolution factor is

$$SR = \tfrac{1}{3} \log_2(1 + E_s/E_n). \tag{5}$$

Here E_s is the signal energy, $E_s = \int_{-\infty}^{\infty} F^2(x)\,\mathrm{d}x$; and E_n is the noise energy, $E_n = n\sigma^2$, where n is the number of experimental data points, and σ^2 is the variance of input noise. If the signal-to-noise ratio is expressed in decibels $\mathrm{dB} = 10\log(E_s/E_n)$, the approximate expression for the superresolution limit is

$$SR \simeq \mathrm{dB}/10. \tag{6}$$

At a signal-to-noise-ratio of about 30 dB (this value is valid for the experimental data discussed below), it follows from equation (6) that $SR \simeq 3$. This means that we can resolve some details in the reconstructed signal at a minimal distance three times better than the size Δ of the instrumental function.

When the signal we want can be described by a formula with a few parameters, the superresolution is determined by the Cramer–Rao inequality [8] and it may be higher than the predicted by equation (5). But when the shape of the spectrum is unknown and the aim of the experiment is to determine the shape, the parametric approach does not work, and resolution is determined by equation (5).

According to the MLM the likelihood function

$$L = \mathcal{P}$$

should be first defined, where

$$\mathcal{P} = \mathcal{P}(F|G_0)$$

is the conditional probability of observing a set of experimental data points

$$F(x_i) \qquad i = 1, 2, \ldots, n$$

which coincides with the real data set, providing that the solution is G_0.

We may consider the set of unknown values of the function $G_0(y_j)$, $j = 1, 2, \ldots, m$ as a vector in an m-dimensional space of solutions. Each point in this space corresponds to one possible solution, and the next step is to search for the likelihood function maximum on a set of solutions limited by some necessary restrictions. For many problems, including those of high-resolution spectroscopy, an important condition is that the solution is not negative. An explicit form of the likelihood function for the case of

polynomial data statistics is given in paper [3]. Poissonian statistics are a special case of polynomial statistics.

If the data are described by Gaussian statistics, then the logarithmic likelihood function is the square of deviation between the experimental data $\{F\}$ and their approximation $\{\hat{F}_0\}$, i.e.

$$\log L = \mathrm{constant} - \tfrac{1}{2}||F - \hat{F}_0||.$$

Here the two vertical lines denote the square norm and $\{\hat{F}_0\}$ is the integral transform (2) of the trial solution $\hat{G}_0$, i.e.

$$\hat{F}_0 = K\hat{G}_0.$$

The search for the likelihood function maximum is performed iteratively by the steepest ascent method which is a sign-inverted variant of steepest descent method. All explicit formulae of iterative algorithms for both polynomial and Gaussian input data statistics can be found in reference [7] and a full listing of the RECOVERY code in Fortran 77 is available from the CPC Program Library providing that persons requesting the program sign the standard CPC non-profit use licence.

The subroutines MLP8, MLG8 or MLU8 are used depending on the noise statistics. The first of these subroutines is intended for input data having Poissonian statistics. The second and the third are designed for data having Gaussian statistics. All three subroutines allow reconstruction of non-negative signals from noisy experimental data distorted by the measuring device.

There are also enhanced versions of the above mentioned subroutines, which use the conjugate gradient method for maximization of the likelihood function instead of gradient one [7]. The ready-to-use (executable) form of this enhanced software for IBM-compatible PCs is available from the second author (ELK). The only difference between ordinary and enhanced versions of the programs is the number of iterations or the computation time and hence it is essential for older PCs, but it is not essential for more powerful Pentium PCs or other new computers.

The data arrays in the upgraded program have been increased to handle 4096 input points in order to allow application of the program to spectra which contain many narrow peaks. The code requires knowledge not only of the kernel $K(x, y)$ of the integral operator (2) but also the input data probability distribution function (PDF). Our measurements have shown that the input data may be described with reasonable accuracy by Poissonian statistics. This is the case because of the type of detector (PMT) we used (see e.g. [9]).

The total number of detected photons in our measurements was about 2×10^5–10^6 for 2048–4096 spectral channels. This gives $\sim$50–500 photons per spectral interval. It is well known [8] that for such great numbers of photons the Poissonian statistics are reduced to Gaussian and we have

$$y = y_0 + \sqrt{y_0} \cdot \mathcal{N}(0, 1). \tag{7}$$

In equation (7) $y = y(i)$ is the observed spectral intensity of light at wavelength $\lambda = \lambda_i$, $y_0 = \bar{y}$ is the unknown mean

value of y at $\lambda = \lambda_i$ and $\mathcal{N}(0, 1)$ is the random variable with Gaussian probability distribution function having

$$\overline{\mathcal{N}} = 0 \text{ and } \sigma^2(\mathcal{N}) = 1.$$

Taking the square root from both sides of equation (7) we have approximately at $y_0 \gg 1$

$$\sqrt{y} \approx \sqrt{y_0} + \frac{\mathcal{N}(0, 1)}{2}. \qquad (8)$$

The residuals between the left- and right-hand sides of equation (8) are shown in figure 3(a) as a function of point number i for the input data presented in figure 4(a) and the PDFs for the residuals in normal (Gaussian) probability scale (see §12 in [10]) are shown in figure 3(b). It is clearly seen from figure 3(b) that the residuals have a Gaussian PDF. From these data we have the estimation

$$\hat{\sigma} \approx 0.385$$

which is a little less than the theoretical value $\sigma = 0.5$ according to equation (8) (see also No 6g.2 in [8]). Such statistics are often observed in spectroscopy for input data obtained by a PMT. In this way we ascertain that our input data have approximately Poissonian statistics. The residuals presented in figure 3 were obtained using the optimal filtering program published in [11].

Since the statistics of the input data are close to Gaussian we may use any one of the subroutines MLP8, MLG8 or MLU8 and still have approximately the same results of recovery. Of course we have to use the correct definition of input data variance in different channels for each from any of these subroutines. The results shown in figures 4 and 5 were obtained using the MLU8 subroutine.

We have to pay some attention here to a problem which occurs in the signal recovery process and is connected with our spectrometer construction. Input data, as a rule, contain a non-constant background resulting from scattering of the analysed light in the spectrometer and from noise in the PMT, the so-called 'dark current'. If the input data contain such a background the program DCONV gives a number of false peaks. After subtracting the background from the input data all false peaks vanish while at the same time the positions of the true peaks do not change. In fact, it turns out to be sufficient to use a constant background for the experimental data shown in figure 4(a).

4. Results

The efficiency of the proposed method for spectral analysis is demonstrated by applying the procedure to the photoluminescence (PL) spectra of excitons bound to the isoelectronic defects B_{18}^1 (1.143 18 eV principle no-phonon line) at helium temperature. It is known that such spectra are reasonably complicated and consist of a number of narrow PL lines with FWHM $\sim$ 30–40 μeV with amplitudes varying over a wide range. The measurements of such spectra permit the evaluation of both the spectrometer quality and the quality of the program for signal recovery, i.e. its efficiency in estimating spectral
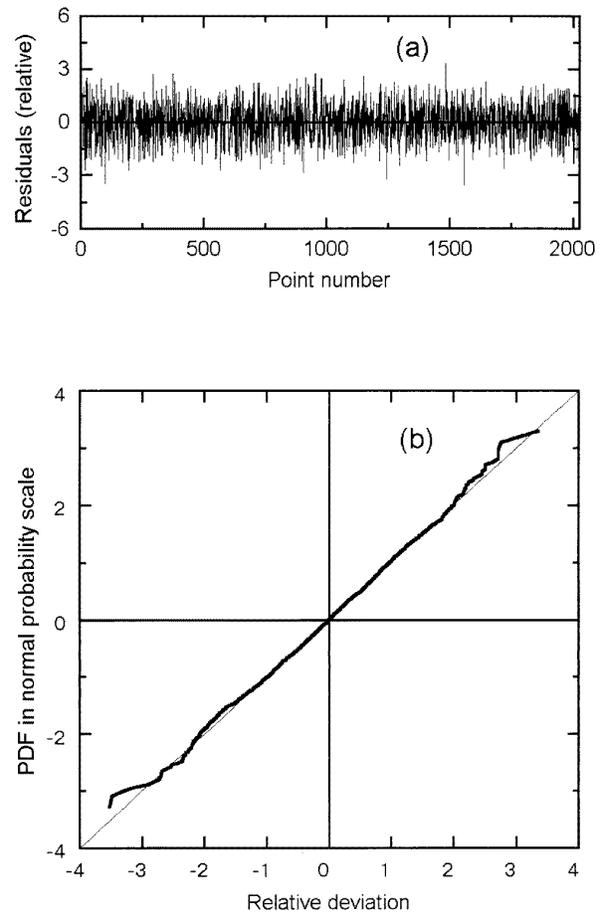

Figure 3. (a) Residuals between the left- and right-hand sides of equation (8) (divided by $\hat{\sigma}$) as a function of point number i for the input data presented in figure 4(a). (b) Probability distribution function for these residuals: the bold curve is the empirical PDF, the thin line is the Gaussian probability integral F. The Y axis is nonlinearly transformed by the formula $F = \int_{-\infty}^{y(F)} 1/(\sqrt{2\pi})\, e^{-x^2/2}\, dx$.

resolution, in investigating the possibility of recovering simultaneously the PL lines of weak and strong intensities, etc.

The PL spectrum of excitons bound to the isoelectronic hydrogen related defects B_{18}^1 in silicon at 4.2 K is shown in figure 4. The samples investigated were produced from a germanium-doped silicon (germanium concentration 3×10^{17} cm^{-3}) grown in a hydrogen atmosphere by the floating-zone technique. The samples were irradiated with a beam of thermal neutrons and then annealed for 30 min in air at 445 °C. The samples were excited by a $\sim$300 mW cw argon laser.

Figure 4(a) shows the PL spectrum recorded by our spectrometer in a mode where the instrumental function, consisting of five narrow peaks (shown in figure 2(c)), corresponds to a monochromator slit width of 0.4 mm. Figure 4(b) shows the PL spectrum which was restored from the spectrum shown in figure 4(a) by the program DCONV. Figure 4(c) shows the same PL spectrum of excitons bound to the centres B_{18}^1 recorded by a BOMEM DA8
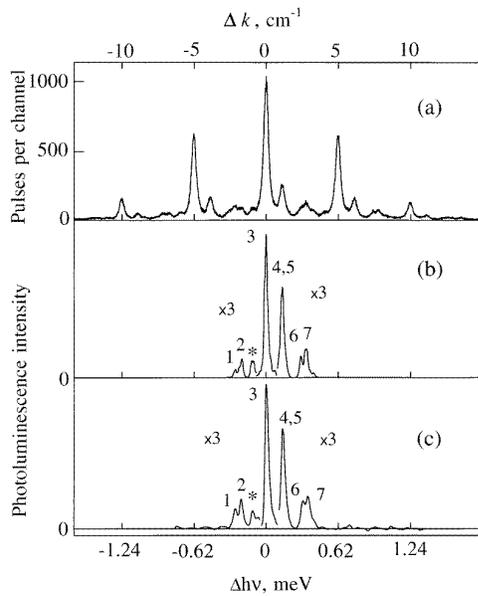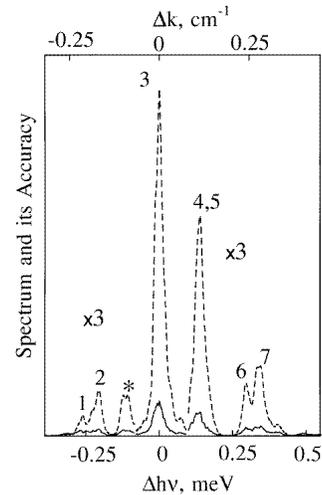
Figure 4. No-phonon PL spectra of excitons bound to the isoelectronic hydrogen-related defects in silicon recorded at 4.2 K. The zero mark on the X axis corresponds to the position of the principal line at 1.143 18 eV. (a) Spectrum recorded with the instrumental function of the spectrometer shown in figure 2(c) (the slit width of the monochromator is 0.4 mm). (b) Spectrum obtained from the spectrum shown in figure 3(a) by applying program DCONV. (c) Spectrum recorded by a BOMEM DA8 Fourier transform spectrometer with resolution 40 μeV (0.32 cm^{-1}). The asterisks mark the main PL line of the excitons bound to the isoelectronic hydrogen-related defects. The main peak (peak 3) in (b) and (c) is scaled down by a factor of three compared to peaks 1, 2, *, 4, 5, 6, and 7.

Figure 5. Spectral density of the PL intensity restored by DCONV (broken curve) and estimation of its accuracy (on the 1σ level) obtained by the Monte Carlo method (full curve). The main peak (peak 3) is scaled down by a factor of three compared to peaks 1, 2, *, 4, 5, 6, and 7 and its position on the X axis corresponds to a principal line energy of 1.143 18 eV.

Fourier transform spectrometer with resolution of 40 μeV (0.32 cm^{-1}) [12].

The full width of the recovered PL spectrum in figure 4(b) equals about 6 cm^{-1}—20% more than distance between the different orders in a Fabry–Pérot interferometer. There is no significant intensity peak of this spectrum which lies outside this range in figure 4(b) and there appear to be weak signals in the Fourier transform (FT) spectrum shown in figure 4(c). This significant difference between these spectra results from the different methods of the signal recovery: we use the nonlinear procedure based on the MLM, which recovers only non-negative signals, whereas FT spectroscopy usually uses the linear procedure based on fast Fourier transform of input data.

It should be noted that FT spectroscopy combined with the nonlinear maximum entropy method of signal recovery [13] can in principle give results similar to ours shown in figure 4(b), however it is not the subject of this paper.

Using equation (3) the resolution of the spectrometer was determined from the instrumental function and turned out to be $\Delta = 34$ μeV. Since a signal-to-noise ratio in this case is about 30 dB it follows from equation (6) that we can resolve some details in the reconstructed spectrum up to 11 μeV. The width of the central peak

(peak 3) in figure 4(b) is 30 μeV. From measurements on a spectrometer with a higher resolution we determined that this is the real width of this line. So it can be easily seen that the procedure of restoration improves the resolution of our spectrometer substantially because the width of the central peak before numerical treatment was 40 μeV.

We can see from this figure the excellent agreement between the spectra recorded directly by a Fourier transform spectrometer with high resolution and those obtained from the input data (given in figure 4(a)) by the program DCONV. From comparison of the spectra presented in figures 4(b) and 4(c), it follows that the proposed method successfully restores the spectrum of analysed light and permits investigation of spectra that contain both strong and weak lines simultaneously. It should be noted that the spectra shown in figure 4(b) and 4(c) are strongly distorted if they are recorded by a well known technique, i.e. using only one order of a Fabry–Pérot interferometer when the monochromator is used as a passive filter. In this case lines 1, 2, 6, 7 could not be resolved because they have approximately the same spectral positions. Moreover, amplitude ratios are also distorted.

The signal-to-noise ratio for the input data shown in figure 4(a) is about 30 dB. We cannot define the signal-to-noise ratio for the output result of recovery by our method shown in figure 4(b), because the intensity values at different points are strongly correlated. In order to evaluate the accuracy of the spectrum restoration we used a Monte Carlo simulation. The estimation of probable accuracy (on the level of 1σ) of the recovered intensity after 50 Monte Carlo trials is shown in figure 5 by the full curve. The broken curve in figure 5 shows distributions of the PL intensity restored by DCONV. The accuracy is about 10% of the values of the restored signal at each

experimental point. This value is about half that of the level of fluctuations of the FT recovered data. So we have proved experimentally that our method gives the correct result of recovery, which is free of the impact of aliasing.

5. Conclusions

The use of a spectrometer with a complicated instrumental function permits the effective solution of problems in high-resolution spectroscopy. In our view it is especially helpful to use instrumental functions consisting of many narrow peaks which do not smooth out the analysed spectrum.

We have demonstrated that the use of a scanning Fabry–Pérot interferometer synchronized with a scanning grating monochromator extends the useful working spectral range of the interferometer considerably and improves its spectral resolution and signal-to-noise ratio. It should be noted that the procedure described above is possible only in conjunction with efficient algorithms for signal reconstruction.

Acknowledgments

References

[1] Mandelstam L 1912 Applications of integral equations to the theory of the optical image *Weber-Festschrift* (Russian transl. 1948 *LI Mandelstam Collected Works* vol 1 (Moscow: USSR Academy of Sciences) pp 229–41)

[2] Tikhonov A N and Arsenin V Ya 1977 *Solution of Ill-posed Problems* (New York: Wiley)

[3] Kosarev E L 1980 Application of the 1st kind integral equations in experimental physics. *Comput. Phys. Commun.* **20** 69–75

[4] Jansson P A (ed) 1984 *Deconvolution with Application in Spectroscopy* (New York: Academic)

[5] Tikhonov A N, Gontcharskii A V, Stepanov V V and Jagola A G 1990 *Numerical Methods of the Ill-posed Problems Solution* (Moscow: Nauka) (in Russian)

[6] Kosarev E L 1990 Shannon's superresolution limit for signal recovery *Inverse Problems* **6** 55–76

[7] Gelfgat V I, Kosarev E L and Podolyak E R 1993 Programs for signal recovery from noisy data using the maximum likelihood principle. Part 1: general description *Comput. Phys. Commun.* **74** 335–48
Gelfgat V I, Kosarev E L and Podolyak E R 1993 Programs for signal recovery from noisy data using the maximum likelihood principle. Part 2: program implementation *Comput. Phys. Commun.* **74** 349–57

[8] Rao C R 1965 *Linear Statistical Inference and its Applications* (New York: Wiley)

[9] Goodman J W 1985 *Statistical Optics* (New York: Wiley)

[10] Hudson D J 1964 Statistics *Lectures on Elementary Statistics and Probability* (Geneva, CERN)

[11] Kosarev E L and Pantos E 1983 Optimal smoothing of noisy data by fast Fourier transform *J. Phys. E: Sci. Instrum.* **16** 537–43

[12] Kaminskii A S, Lavrov E V, Davies G, Lightowlers E C and Safonov A N 1996 Isoelectronic hydrogen-related defects in silicon *Semicond. Sci. Technol.* **11** 1796–803

[13] Kawata S, Minami K and Minami S 1983 Superresolution of Fourier transform spectroscopy data by maximum entropy method *Appl. Opt.* **22** 3593–8